Optimal Design of Shunt Active Power Filter for Power Quality Improvement and Reactive Power Management Using nm-Predator Prey Based Firefly Algorithm

Devi Prasad Acharya*, Subhashree Choudhury**‡, Niranjan Nayak***

*Department of EEE, Research Scholar, SOA Deemed to be University, ITER

**Department of EEE, Associate Professor, SOA Deemed to be University, ITER

*** Department of EEE, ITER, Professor, SOA Deemed to be University, ITER

(deviprasad049@gmail.com, subhashreechoudhury@soa.ac.in, niranjannayak@soa.ac.in)

‡ Devi Prasad Acharya; 751019, Tel: +91 8328953908, deviprasad049@gmail.com

Received: 05.01.2022 Accepted: 10.02.2022

Abstract- The utilization of the modern power electronics equipment causes fluctuation of loads which is the cause of distortion of normal sinusoidal pattern of the current and voltage waveforms thus leading to disturbances in the system known as harmonics. These disturbances are the main factor of overheating the equipment, reducing the efficiency and thus damaging the system equipment. Here in this paper a Shunt Active Power Filter is designed to eliminate the harmonics in a power system in grid connected mode of operation. The SAPF is integrated with a PI-controller whose parameters are taken randomly. This creates a challenge to improve the filter performance. Here different types of optimization methods are utilized to obtain optimized gains of the PI-controller parameters. There are many conventional methods for the selection of controller parameters as well as filter parameters where the parameters are optimized for the elimination of harmonics. This work intends to eliminate the Total Harmonic Distortion (THD) with the help of proposed nm-Predator Prey Fire-Fly Algorithm (nm-PPFO). Also other conventional methods such as Gravitational Search Algorithm (GSA), Particle swarm Optimization (PSO) and Accelerated PSO have been implemented. Predator Prey based firefly optimization (PPFO) is taken into account for better response. Proposed nm based predator prey algorithm (nm-PPFO) is simulated and compared with above discussed optimization processes. Apart from THD, the power factor is also calculated and compared for various operating condition. The system is designed using Matlab-Simulink environment and the results found out justify the robustness of the proposed method as compared to other techniques in reducing the harmonics effectively.

Keywords Shunt Active Power Filter (SAPF), Total Harmonic Distortion (THD), Gravitational Search Algorithm (GSA), Predator Prey Based Firefly Algorithm (PPFO) and nm-Predator Prey Fire-fly Algorithm (nm-PPFO).

1. Introduction

The extensive utilization of modern power electronic devices cause disturbances in the power system network due to their switching nature, which is the root cause of harmonics in the system. Due to the presence of nonlinear loads and reactive power components, harmonics of current are being drawn from the main supply. The basic cause of current harmonics is due to adjustable speed drives, Static Compensators (STATCOM), Switch Mode Power Supply (SMPS) and Uninterrupted Power Supplies (UPS). The harmonics are the basic cause of equipment malfunction and overheating, capacitor bursting, unwanted vibrations in motors and poor power factor. In conventional practice, passive LC or RLC filters are being used for mitigation of harmonics present in the system, but these devices are associated with problems like bulky and static nature of capacitor banks and resonance [1]. Further the compensation is of constant magnitude and cannot be varied from time to time along with load variation.

The active power filters work on the basis of injecting an appropriate reimbursing current at the point of common coupling (PCC) .The active power filter delivers a current of same magnitude, but contradictory phase to the harmonic component drawn by the nonlinear loads. Thus only after cancellation of the harmonic affects, it draws only fundamental component of current from the supply. For more accurate operation of SAPF it requires quick estimation of the harmonic component of the load current. Artificial Neural Network (ANN) based controller is used for faster calculation and suppression of THD of source current [2-3]. The modified compensating strategies including balanced and sinusoidal source current having unity power factor, are applied to a real time power network [4]. The performance of SAPF in case of a three phase four wire system is analyzed and discussed to reduce the neutral current and zero sequence component for the minimization of harmonics in a single phase system [5]. In [6] the authors have emphasized on the use of recursive least square (RLS) technique for detecting the harmonics and its mitigation with a SAPF with an upgraded current control method in a power system network affected by distortions. RLS method is simple, accurate and has quick convergence characteristics. Utilization of Superconducting Magnetic energy Storage (SMES) based SAPF is designed and modelled in [7] for efficient compensation of varying load demands and transient power fluctuations. Here Modified Synchronous Reference Frame (MSRF) method has been utilized to produce appropriate gate pulses for the Voltage Source Converter (VSC) of the SMES connected to the SAPF of the three phase system. Authors have discussed the application of Dynamic Voltage Restorer (DVR) in [8] for elimination of swell and sag condition in power network. Instantaneous reactive power theory along with a two-level Voltage Source Inverter (VSI), is used for estimation of references harmonic currents [9] for a grid connected SAPF. A simple control technique is proposed in [10] for three-phase shunt active filters where computation of the reactive current component is not necessary and direct control of reactive current is introduced. Use of serial active power filters is proposed in [11] for line conditioning in case of distributed power networks. Reference compensating currents are generated based on the balance of the active and reactive power generated in the SAPF instantaneously is proposed in [12]. In the above mentioned research application the filter parameters are chosen arbitrarily which influences the working and stability of the system. Also performance of SAPF is mostly affected by the generation of reference voltage or current which depends on the PI controller gain of the SAPF. The authors in [13] have proposed a Differential Evolution Optimization (DEO) technique and artificial neural network (ANN) based PI-controller for controlling the frequency and voltage at steady-state conditions of a micro grid with distributed resources. The Intelligent Adaptive Control method of the SAPF for enhancement of micro grid power quality has been performed in [14]. The minimization of power quality issues like fluctuation in frequency and voltage with the help of smart power electronic equipment has been suggested in [15]. In [16] the enhancement of power quality issues of the smart micro grid system has been performed with the use of shunt hybrid filters.

The conventional method of tuning the PI controller parameters involves linear modelling and leads to non-optimal tuning of parameters [17]. Differential evolution (DE) is a proficient search method for solving complicated optimization programs over uninterrupted space [18] and based on population. In [19] researchers have used fuzzy logic controllers (FLC) to modify the required parameters for crossover and mutation operations. Artificial Neural Network (ANN) based optimization is used for the effective and highly predictive back propagation technique as proposed in [20].

There are many advanced evolutionary optimization algorithms based on swarm intelligence such as Genetic Algorithm (GA) [21], Bacterial Foraging (BF) [22], Bacterial Foraging with Swarming (BFS)[23], Particle Swarm Optimization (PSO)[24]. For solving dynamic optimizing operations complicated optimization problems algorithms techniques such as ant colony optimization (ACO) [25] is used. The nature inspired gravity dependent Gravitation Search Algorithm (GSA) for solving complex problems is proposed in [26]. Further the more accurate and advanced version of PSO known as Accelerated PSO (APSO) is proposed in [27] where acceleration is up-dated along with that of position and velocity unlike that of PSO. For dealing with the power quality problems associated with Hybrid Renewable Energy Source (HRES) system, Atom Search Optimization (ASO) has been proposed for optimizing the Unified Power Flow Controller (UPQC) [28]. The popular Squirrel Search Algorithm (SSA) and PSO has been used to optimize the PID controller parameters for a multilevel H-bridge based multilevel inverter [29]. Hybrid optimization technique has been utilized to optimize the PI controller gains of a SAPF connected to a grid-tied PV based micro grid system [30]. The optimal power flow has been addressed using of an improved artificial bee colony algorithm (ABC) with Global and Local Neighbourhoods (ABCGLN) [31]. The hybrid optimization technique like PSOGSA has been adopted to optimize the power flow and minimize the operational cost in a hybrid micro grid involving a PV array, wind, diesel, and battery storage unit [32].The unceasing power flow study is investigated in a IEEE-14 bus system [33] using FACT devices like SVC (Static Var Compensator), UPFC (Unified Power Flow Controller), STATCOM (Static Synchronous Compensator) and SSSC (Static Synchronous Series Compensator). The reimbursement technique involving unbalanced voltage through real, reactive power regulation by utilizing a smart inverter has been suggested in [34], which improves the voltage unbalance index and detects the unbalance in both phase and amplitude of voltage, and thereby improving the quality of power.

Most of the above discussed optimization techniques optimize the PI controller gain parameters only without affecting the other important parameters of SAPF like the filter inductance, filter resistance, DC side capacitance and the dc reference voltage. But for the optimal operation of the SAPF, the parameters other than that of PI controller gains must be optimized keeping in aim for improvisation of the power quality of the system.

In this research work a SAPF is considered for a grid connected system with non-linear load and various optimization techniques like GSA, PSO, PPFO and nm-PPFO are programmed to choose the best values of PI controller gains and some of the filter parameters.

The literature review suggests the firefly optimization is more efficient in optimizing the SAPF parameters as compared to traditional PSO and GSA algorithms as it takes less number of iterations. So in this study the Firefly optimization method is modified to make the SAPF controller more robust in minimizing the power quality issues of the proposed micro grid.

The remaining portion of the study is arranged as described. The System model is elaborated in Section II. The conventional and proposed Optimization techniques are illustrated in Section III. The results and discussions are presented systematically in Section IV. At last the Conclusions from the entire study has been given in Section V.

2. System Model

Here the model of a grid connected power system with SAPF is considered for study. A three phase source or generator, a short transmission line, a three phase transformer and a utility grid along with a SAPF are the constituents of the model. The use of nonlinear load, power electronics devices produces different power quality issues among which the harmonics is a challenging issue. In this work major focus has been given to the design of SAPF, based on various types of optimization techniques and its performance is compared under different operating conditions.

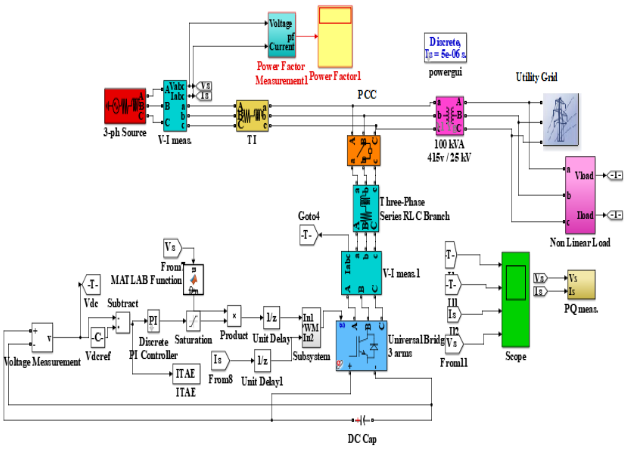

Fig. 1. System Model

Figure-1 depicts the proposed system which consists of a 3 phase source connected to a nonlinear load and grid through a transformer. At the point of common coupling (PCC) the Shunt Active Power Filter (SAPF) is connected through a three phase breaker. The SAPF can be either connected or disconnected from PCC at any time depending upon the requirement of the system.

2.1 Grid

The grid is designed as two feeder lines first one a 5 km feeder and second one, a 14 km feeder line intervened with a 2 MW load. The 14 km feeder is 125 KV, 2500 MVA source through a120 kV/25 KV star delta transformer whose primary star side neutral point is grounded. A 30 MW, 2MVAR load is coupled after the 14 km feeder line. Also a 25 KV grounding transformer is connected before the transformer to the ground through a 3.3 Ω resistor.

2.2. Shunt Active Power Filter (SAPF)

Generally filters are utilized to reduce the disturbances produced due to repeated switching of power electronics devices. The SAPFs are installed parallel to the load as the harmonics arising due to load are needed to be eliminated or minimized. The SAPF works by detecting the harmonic current in the load side and affords a current of equivalent magnitude and contradictory phase and injects the same at the PCC. The SAPF also controls the reactive power in the system by eliminating the harmonics. Hence it is more suitable than that of series active power filters in its working and functions.

The choosing of SAPF parameters is of prime importance. Coupling inductor L_f , dc capacitor C_{dc} and dc reference voltage can be chosen assuming; 1) proper sinusoidal source current; 2) the maximum distortion allowed for the AC line current must be within 5% and 3) inverter operates in a linear modulation mode. The parameters L_f and V_{dc} can be fetched as follows:

$$Q_c = 3V_c I_c = 3V_s \frac{V_c}{\omega L_f}\left(1 - \frac{V_s}{V_c}\right) \tag{1}$$

$$I_h = \frac{V_h}{m_f \omega L_f} \tag{2}$$

V_{dcref} is the reference dc voltage and C_{dc} is nominated as follows:

$$C_{dc} = \frac{\pi^* I_c^{rated}}{\sqrt{3}\ \omega V_{pp}^{ripple}} \tag{3}$$

Where V_c = compensated voltage, L_f coupling inductance of SAPF, C_{dc} = DC side capacitor of the filter, V_S = source voltage of SAPF, I_c compensated voltage and V_h is the harmonic voltage.

2.2.1. *Design of SAPF*

The SAPF with VSI injects a reimbursing current at the PCC which makes the source current free from contortion.

Also it makes the current in source side and source voltage are in phase without affecting the properties of the load, as denoted in Figure.2. Following equations describes the instantaneous nature of source current, load current and load power which can be mathematically represented as

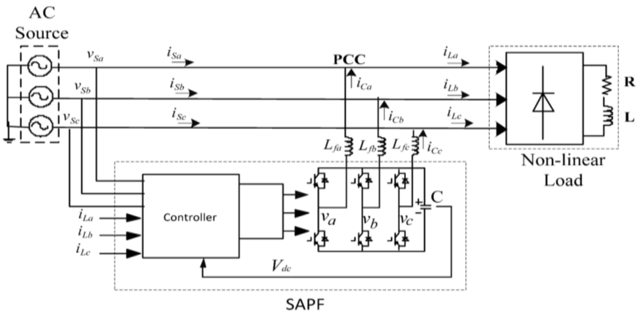

Fig. 2. Block Diagram for SAPF circuit

$$i_{source}(t) = i_{load}(t) - i_{filter}(t) \tag{4}$$

$$v_{source}(t) = v_{\max} \sin \omega t \tag{5}$$

$$i_{load}((t) = \sum_{m=1}^{\infty} I_n \sin(m\omega t + \phi_m) \tag{6}$$

$$P_{lolad}(t) = v_{source}(t) * i_{load}(t) \tag{7}$$

The instant load power $P_l(t)$ consists of the basic component of active Power $P_f(t)$, harmonic power along with reactive power. An appropriate atoning current has to be inserted at the PCC, which lets the source current to have only the basic portion of the load current as given in Equation (8), for the SAPF to be controlled effectively.

$$i_{source}(t) = \frac{p_{fund}(t)}{v_{source}(t)} = I_1 * \cos\phi_1 * \sin \omega t = I_{sm} * \sin \omega t \tag{8}$$

The peak source current also contains capacitor leakage loss component and switching losses associated with the inverter of the SAPF as given by

$$I_{sp} = I_{sm} + I_{sl} = I_1 \cos\phi_1 + I_{sl} \tag{9}$$

The shunt active filter must inject appropriate reactive component of the load harmonic current aiming for making the source current pure sinusoidal which will be in the same phase as that of the source voltage which can be represented mathematically as:

$$i_{fund}(t) = i_{Load}(t) - i_{source}(t) \tag{10}$$

After SAPF injection the modified source currents are denoted as follows:

$$i_{sa}^* = I_{sp} * \sin \omega t \tag{11}$$

$$i_{sb}^* = I_{sp} * \sin(\omega t - 120) \tag{12}$$

$$i_{sc}^* = I_{sp} * \sin(\omega t + 120) \tag{13}$$

In the above equations and wave shapes of I_{source}, the phase angles are given but the amplitude of I_{source} must be calculated. For this purpose dc capacitor voltage is equated with a fixed reference value for the generation of an error signal. This PI controller receives this error signal, and magnitude of desired I_{source} is calculated. The estimated currents which are in phase with source voltages are multiplied with unit sign vector components.

2.2.2. Design of Gain Parameters

The voltage characteristics and damping ratio of the PI controller are denoted by the gains K_p and K_i. The quality equation of the voltage maintenance loop shows these parameters as given below:

$$1 + (k_p + \frac{k_i}{s} + k_d s)C_{dc} = \frac{3[v_{source} - sl_f I_\omega - 2I_\omega R_f]}{sC_{dc} v_{dc0}} = 0 \tag{14}$$

2.3. Nonlinear Load

The nonlinear load is a branch that is attached to the grid in parallel and consists of either of R, RL, RLC load, rectifier load or a dynamic load connected to a bus through a three phase breaker. Each load discussed above is connected to the bus with a three phase breaker, so that at any time the loads can be connected according to our convenience and requirement. The load voltage and load current are being calculated from the bus terminals. Figure-3 illustrates the nonlinear load considered in this study.

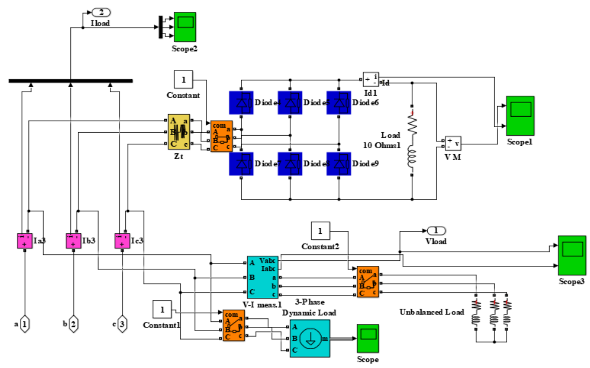

Fig. 3. Nonlinear load

3. Optimization Techniques

The design of SAPF has a vital part in harmonic suppression of a power system. The filter parameter selection along with PI controller gains is random, which affects the performance of SAPF. Thus different optimization algorithms as GSA, PSO, PPFO and nm-PPFO are executed to achieve optimal values of $K_p, K_i, L_f, R_f, C_{dc}$ and V_{dcref}.

3.1. Particle swarm Optimization (PSO)

PSO is based on collective behaviour of animals such as flocking of bird .The basic theme of PSO is to replicate a flock of birds in search for nutrients. PSO has quick rate of convergence in comparison to other traditional techniques. In PSO parameters are required to be controlled as compared to others so implementation is much easier. This algorithm can be designed to optimize multi-dimensional or multi variable optimization programs. Each element of swarm (called particle) has a velocity and a position of its own. These elements move inside a complex search space aiming for a feasible solution. Every element modifies its position in the exploration space repeatedly according to the flocking involvement of it along with its neighbours. The mobility of every element is determined by the two equations given below, inside the exploration space [24].

$$v_{ij}^{t+1} = wv_{ij}^{t} + c_1 rand_1 (p_{bestij}^{t} - x_{ij}^{t}) + c_2 rand_2 (g_{bestij}^{t} - x_{ij}^{t}) \quad (15)$$

$$x_{ij}^{t+1} = x_{ij}^{t} + v_{ij}^{t} \quad (16)$$

Here x_i is the current position of the element I; v_i is the speed of element i ; P_{besti} is particle best of element i , G_{best} Represents group best for the entire population; $rand_1$ and $rand_2$ are two random vectors in the range [0 1]; w is a weight of inertia; C_1 is cognitive factor and C_2 is the social factors of learning.

3.2. Gravitational Search Algorithm (GSA)

GSA is a population based exploration process [26] .It is dependent upon Newton’s Law of Gravitation and relates to mass interconnections. The results in the GSA community are known as agents which link with one another with the help of gravitational force. The execution of every element in the community is dependent upon its mass. Every element is taken as an entity and they move towards others of higher mass according to law of gravitation. The objects of larger mass move very slow which is represented as the exploitation step of GSA.

At any time‘t’ the gravitational constant G is calculated as given below:

$$G(t) = G_0 \times e^{-\alpha t / T} \quad (17)$$

Here G_0 and α represent constants and their initialization is done at the start of algorithm, whose magnitudes will be minimized during the exploration. ‘T’ denotes number of iterations used in the process.

The agents are obey the law of gravitation as given below:

$$F = G \frac{M_1 M_2}{R^2} \quad (18)$$

Where F represents the gravitational force of attraction; G = Universal gravitational constant; M_1 and M_2 = masses of the elements; R = distance joining the two elements.

According to Newton's second law, whenever a force F is acted upon an element, the element travels with an acceleration a which is dependent on the force applied and the mass of element M as given in equation (19)

$$a = \frac{F}{M} \quad (19)$$

Three types of masses are considered:

Active gravitational mass M_a ; Passive gravitational mass M_j ; Inertial mass M_i

The force of gravitation F_{ij} that operates on $i'th$ mass by $j'th$ mass is given by equation (20):

$$F_{ij} = G * \left(\frac{M_{aj} * M_{pi}}{r^2}\right) \quad (20)$$

Here active mass of element $j = M_{aj}$, passive mass of object $i =. M_{pi}$

Acceleration of any object i is given as

$$a_i = \frac{F_{ij}}{M_{ii}} \quad (21)$$

Where M_{ii} is the inertial mass of $i'th$ element

The agents renovate their velocities and positions as given in Equations (22) and

$$vel_i^{t+1} = rand_i * vel_i^t + a_i^t \quad (22)$$

$$x_i^{t+1} = rand_i * vel_i^t + a_i^t \quad (23)$$

Steps of the GSA

Step-1: Initialize merits of gravitational constant G0, α, ε and the counter of iteration t.

Step-2: Generate random primary population initially which comprises of N objects where location of each object is denoted as

$$X_i(t) = (x_i^1(t), x_i^2(t), x_i^3(t) \ldots\ldots\ldots\ldots x_i^d(t), \ldots\ldots x_i^n(t)), i = 1,2,\ldots\ldots N \quad (24)$$

Step-3:.Repeat the following sequence until desired termination criterion is satisfied

Step-4: Calculate every object in the population and assign best and worst agents. The gravitational constant is modified as given in equation.

Step-5: for a given time't' the force which element j acts on element i, can be evaluated as follows

$$F_{ij}^t = G^t \frac{M_{pi}^t \times M_{aj}^t}{R_{ij}^t + \varepsilon}(x_j^t - x_i^t) \tag{25}$$

Step-6: The net force exerted on element i is given as

$$F_i^t = \sum_{j \in kbest, j \neq i} rand_j F_{ij}^t \tag{26}$$

Here K_{best} represents best fitness values of initial K elements.

Step-7: The inertial mass can be calculated as follows

$$m_i(t) = \frac{fit_i - worst(t)}{best(t) - worst(t)} \tag{27}$$

Step-8: The gain in momentum of $i'th$ is evaluated as

$$a_i^t = \frac{F_i^t}{M_{ij}^t} \tag{28}$$

Step-9: For any agent i the velocity and displacement factors are modified as given in Equations (22) and (23).

Step-10: Increase the iteration counter until satisfaction of the termination criteria satisfied.

Step-5: Required best optimal solution is evaluated.

3.3. Firefly Optimization (FFO) Algorithm

Firefly optimization is inspired by the luminescent behaviour of flash bugs which are otherwise known as fireflies [35, 36, 37, and 38]. The randomly generated feasible solutions are considered as fireflies whose brightness are estimated by the performance of their objective functions. There are three guidelines for this algorithm:

1. Flies are androgynous, which inspires that any fly can be allured by other fireflies.

2. Brightness of a fly is dependent upon the performance of its objective function.

3. Attraction of a firefly depends upon its brightness which diminishes with increase in distance.

The light intensity follows inverse square rule as given in equation (29)

$$I \alpha \frac{1}{r^2} \tag{29}$$

Where I is the intensity of light and r is the space interval. The brightness also follows same rule. When the light is passing through any medium of absorption coefficient γ, the brightness of any firefly over a distance r is given as:

$$\beta = \beta_0 e^{-\gamma r^2} \tag{30}$$

Where β is the brightness of a fly over a distance r and β_0 is brightness at source point, (r =0).

A firefly x_i moves towards another firefly x_j using the rule given below:

$$x_i^* = x_i + \beta_0 e^{-\gamma r_{ij}^2}(x_j - x_i) \tag{31}$$

In addition to this the firefly searches the random space given by equation:

$$x_i^* = x_i + \alpha(rand() - 0.5) \tag{32}$$

Where α denotes the step length and $rand()$ is an 'N' dimensional vector ranging between [0 1].

Updating the movement of firefly x_i we have

$$x_i^* = x_i + \beta_0 e^{-\gamma r_{ij}^2}(x_j - x_i) + \alpha(rand() - 0.5) \tag{33}$$

So there are basically two types of movements of fireflies, mutual attraction and random movement .But if a firefly cannot find another brighter firefly, it will only have to perform the random movement.

Steps in FF Algorithm:

Step-1: Arbitrary solutions are generated, $\{x_1, x_2 .... x_k\}$

Step-2: Intensity of every member in the solution must be computed. $I_1, I_2, I_3 ...... I_k$

Step-3: Each firefly moves towards the brighter fireflies in case of unavailability of brighter firefly then they take random direction.

Step-4: Upgrade the set of solution.

Step-5: Abort when conclusion norm is fulfilled else go back to step 2. Continue till criterion is met

3.4. Predator Prey Based Firefly Optimization (PPFO) algorithm

Predator Prey Firefly optimization is based on behaviour of animals, who work together to solve complex problems. This technique is based on flashing pattern of fireflies. Each firefly has unique flashing pattern. The attractiveness among fireflies is directly related to their brightness, which decrease with increase in distance. [39, 40, 41]

The SAPF is basically used to insert an appropriate reimbursing current at PCC aiming for modifying the source current properly sinusoidal with minimum Total Harmonic Distortion (THD). The inserted waveform of current and the distortion of the evolving current source is dependent upon parameters of filter. Hence designing of proposed filter can be worked out as a modification issue where minimization of the THD should be the main objective. This target can be achieved through optimally choosing the model parameters. This work unites the Firefly Optimization with predator-prey technique for enhancing the search and manipulation capabilities during the exploration, which is applied in designing the SAPF for optimal results. The firefly algorithm is based on the flashing behaviour of flies, whereas the Prey and Predator method is motivated from stalking activity of predators towards another swarm of small animals known as preys. The suggested work demands demarcation of model variants and optimizing these variables for a better result. The model variants of the filter taken here are $L_f, R_f, k_p, k_i, C_{dc}$ and $L_f, R_f, k_p, k_i, C_{dc}$ v_{dcref}. Initially a flock of flies are arbitrarily populated and each fly represents a feasible remedy for the problem exploration room and the room dimension is same as the number of model variants. Suggested work represents each fly ∂fp for selecting the model variables as given below:

$$f = [L_f R_f k_p k_i C_{dc} v_{dcref}] \quad (34)$$

Which is constrained by equation (35)

$$f_k(\min) < f_k < f_k(\max) \quad (35)$$

The phenomenon of bioluminescent communication is used in the algorithm to control the motion of the fireflies in the search area. Every fly is lured towards the luminescence of other flies, hence starts to travel in their direction. The luminescence of fireflies are attached with the execution of the formulated scheme issue. In each iteration the method determines the relative force of attraction and brightness level of every fly, further the positions of the flies are updated with the help of these entities. The function (β_{fun}) which denotes brightness is written to lower the harmonics present in the source current as given below:

Magnify

$$\beta_{fun} = \frac{1}{1+thd} \quad (36)$$

Phenomenon of attraction between the two fireflies i and j and β_{ij} is denoted as follows:

$$\beta_{i,j} = \beta_0 \exp(-\gamma d_{ij}^2) \quad (37)$$

Where d_{ij} represents the displacement between fireflies i and j respectively, and can be calculated as:

$$d_{ij} = \| f_i - f_j \| = \sqrt{\sum_{k=1}^{nd} (f_i^k - f_j^k)^2} \quad (38)$$

Inside the flock, fly i travels in the direction of fly j and renovates its present location, if β_{funj} is larger than β_{funi} at interval t:

$$f_i^t = f_i^{t-1} + \beta_{ij}(f_j^{t-1} - f_i^{t-1}) + \alpha(rand - 0.5) \quad (39)$$

Each firefly (prey) is hardly confined to its formal location when pursued by a predator and opt for updated positions which is away from reach of predator flies. The stalking action of predator fly allows it to traverse along the problem space area in a more accurate manner. Predators control their stalking process by a factor η known as hunting factor. The predators are modelled mathematically on the worst value of solutions given by:

$$f^*_{predator}(t) = f^*_{worst}(t) + \rho(1 - \frac{t}{T_{\max}}) \quad (40)$$

The behaviour of flies frequently lets them from the reach predators, and mathematically modelled as given by equation below:

$$f^{t+1} = f^t + \rho.e^{|-d|}, if d > 0$$
$$f^{t+1} = f^t - \rho.e^{|-d|}, if d < 0 \quad (41)$$

$$\mathrm{PF} = \cos\theta * \left(\frac{1}{\sqrt[2]{(1+THD^2}} \right) \quad (42)$$

This PPFO never allows the flock to converge to non-optimum point in the process of exploration, but boosts the ability of search process and makes the iterations to meet at the global best point. The process of exploration starts as random values are generated within their constraints for individual firefly and β_{fun} value is estimated by simulating the proposed model as shown in Fig.1. Based on the value of β_{fun}, the fireflies move towards the brighter ones which denotes better optimal solution. The fireflies hunt probabilistically in form of predators, and hence fireflies break free from the suboptimal entrapment. The iterations are performed till convergence is reached.

3.5. nm- Predator Prey Firefly Algorithm (nm-PPFO)

During searching for global solution, sometimes it trapped into the local optimal Solution. To overcome this strength of investigation must be large enough which affects the convergence rate of the algorithm. In the previous algorithm predator n explores its boundaries and also lets other preys to move inside the problem space with statistically. The inspection characteristics of the algorithm is inspired by picking up several predators [42]. Degree of searching can be increased by maximizing the best predators count from 1 to n and the quality of searching by increasing best prey count starting from 1 up to m. A quality searching behaviour for robust algorithm requires higher n value. For deviating problems and to find many local and global solutions the value of m should be increased. For Obtaining best stopping requirements the bet preys and predators are to be modified.

Sole tampering in the process of the general prey is, if the possibility of repetition, P_f is not achieved, the prey will move away from the worst predator. Thus essential steps of the planned algorithm are as follows in the flow chart.

Step-1: Generate N random solutions.

Step-2: Solutions are to be arranged in ascending order as per their performance in the objective functions.

For example $y_1, y_2, y_3 --y_n$, $f(y_i) > f(y_{i+1})$

Here $\{L_f, R_f, K_p, K_i, C_{dc} and V_{dcrref}\}$

Step-3: Arrange the solutions as predator $\{y_1, y_2, y_3........y_n\}$, ordinary prey $y_{n+1}, y_{n+2}, ---y_{n-m}$ and best prey $\{y_{N-m+1}, y_{N-m+2}..........y_N\}$

Here in our problem, ordinary prey is $\{L_f, R_f, C_{dc}, V_{dcref}$ and the best prey is $\{K_p, K_i\}$

Step-4: Let the predators move in a random manner and in the direction of y_{n+1}

Step-5: Let the general prey travel in the direction of $y_{i+1}, y_{i+2}, -- y_n$ if $Rand < P_f$ for a random number rand, else, displace y_i arbitrarily away from y_1 .

Step-6: Proceed every best prey y*b* with random *q* and in an updated direction.

Step-7: If conditions for winding up is obtained, end; else, move to step -2 again.

The technique is recapitulated as in Fig.4. The criterion for conclusion may be the maximum number of iterations, no correction is obtained in successive generations for a tolerance level given is archived if the best solution is known.

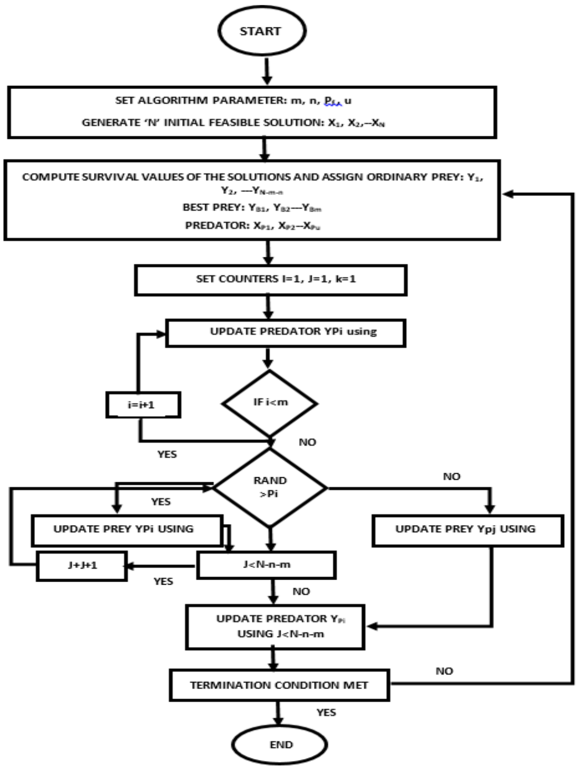

Fig. 4. Nm-Predator prey optimization flow chart

4. Results and Discussions

The suggested SAPF is designed and simulated in Matlab/Simulink domain. The model is successfully simulated for different optimization methods and the harmonic distortions are calculated. The three phase waveforms for different cases for the nm-PPFO technique are given in Figure (5,8,11,14and 17) as well as the harmonic distortions were calculated for load current and source current which are presented in Fig (6,7,9,10,12,13,15,16,18 and 19). Five test cases are considered for the proper verification of the Model which are given in Table-1. The different parameters used are specified in Table-2. All the test cases were successfully simulated with different results and the THD variation for all the test cases are given in tabular form for load current(Table-5) and source current(Table-6). The source side power factors are calculated and compared in Table-7 for all the test cases considered, with different optimization techniques taken into account. Six parameters are optimized in different optimization processes, whose boundary (Upper and Lower) values are given in Table-3.The optimized values of these decision variables which are modified to reduce the THD are calculated and are given in Table-4 for different optimization processes for different test cases. No assurance can be suggested for multiple implementation of the nm-predator prey optimization technique converge to constant solution because of the varying behaviour of the flock optimization technique. So the process has been implemented 17 times and the better solutions have been represented. The model has been optimized for multiple test instances such as without SAPF, SAPF with Conventional PI controller [28], SAPF with GSA, SAPF with PSO [29], SAPF with PPFO and SAPF with nm-PPFO .

Table-8 represents the optimized values for different design parameters which are obtained by different optimization techniques. Here the optimized parameter for nm-PPFO, PPFO, GSA and PSO are denoted for different test instances. The THD values are being calculated at the PCC before and after connecting SAPF.

The current in the load side is almost unbiased and sine wave with a distortion of 7.48% in CASE-1 and with a PF of 0.9658.The SAPF is able to minimize the THD further to 1.9902%. This value is very less as compared to that of conventional methods as shown in Table-6. Here the power factor is also enhanced to unity (0.9996). The sinusoidal nature of source current can be seen in Figure-5. The source current THD is 2.23% and is reduced to 0.76% after connecting the SAPF.

The load current in CASE-2 is balanced but not perfectly sinusoidal as shown in Fig-8, with a THD of 5.07% and a poor power factor of 0.8995 in one phase. With a proper injection from SAPF the THD value is decreased to 4.33%. After the injection of reactive power form SAPF the Power factor is also increased to 0.9432.

In CASE-3 and CASE-4 the load current THD are 5.45% and 8.91% respectively. Again after connecting the SAPF the THD values are decreased to 4.33%. The power factor before connecting SAPF are 0.8995 in one of the phase in case-3 and as lower as 0.8805 in CASE-4. After the application of SAPF along with nm-PPFO the power factor values are being increased to 0.9954 and 0.9726 respectively. Correspondingly the source current THD are also being reduced as given in Table-7.

In CASE-5 where a dynamic load is connected with the system the load current THD value is as large as 8.07% with a power factor of 0.8991 in one of the phase. The SAPF along with nm-PPFO is efficient to minimize the THD to 5.22%. The power factor after connecting SAPF is improved and given by 0.9987. The source current THD has a value of 4.01 before connecting the active filter and 2.55% after injecting reactive power from SAPF.

Figure-20 represents the harmonic spectrum for CASE-3. It can be verified that 5-th, 7-th and 9-th harmonics are large while other harmonics are negligibly small.

The values of R and L are changed proportionately and the harmonic distortion values of the results are calculated which are given graphically in Figure-21 for rectifier load, which denotes the performance of the proposed model for different load levels. From the figure it is ascertained that the harmonic distortion is minimum (2%) for load factor of 1.55 and below, which depicts the excellent operation of nm-predator prey optimization for load variations. But when the load factor is found to be more than 1.55, the SAPF is not effective.

Value of THD is calculated for all the discussed five test cases 1, 2, 3,4and 5, where the values are found to be lower than 9%. The maximum allowed harmonic distortion limit is 5% as per IEEE 519–2014 standard. From the results and tabulations it is pretty clear that nm-PPFO can minimize the harmonic distortion level to within 5% and hence following the IEEE 519–2014 standard restriction of 5% and making sure sinusoidal load current and Source current. Nm-PPFO is found to be the best optimization process for reduction of THD.

The convergence characteristics for various optimization techniques are presented in fig-22.The convergence curves are drawn for GSA, PSO, FFO, and nm-PPFO. From figure it can be seen that the proposed nm-PPFO algorithm converges faster as compared to other optimization techniques used. The developed technique takes lesser number of iterations (26) to converge which is less as compared to others as shown.

Table 1. Test cases considered

TEST CASES	SOURCE	LOAD TYPES
CASE-1	3-Phase Balanced	3-Phase Rectifier Load
CASE-2	3-Phase Balanced	3-Phase R- Load
CASE-3	3-Phase Balanced	3-Phase RL- Load
CASE-4	3-Phase Balanced	3-Phase RLC- Load
CASE-5	3-Phase Balanced	3-Phase Dynamic Load

Table 2. Parameters utilized

Parameter	value
nf	30
βo	0.97
γ	0.92
α	0.5
η	0.02
T_{max}	150
P	0.045

Table 3. Boundary values for variables

Variants	k_p	k_i	C_{dc} (μF)	v_{dcref} $(volt)$	L_f (mH)	R_f (Ω)
LB	0.001	0.001	400	600	0.01	0.0001
UB	100	100	5000	1500	10	0.5

Table 4. Values of Variables for different optimization techniques

Methods	k_p	k_i	C_{dc}	v_{dcref}	L_f	R_f
CONV-PI	0.57	10.3	2000	220	0.66	0.1
GSA	54.7009	20.7743	610.48	517.4380	6.059	0.1460
PSO	53.0865	96.8649	460	427.7639	4.20	0.3499
PPFO	39.735	39.735	4100	1345.8	9.05	0.4399
nm-PPFO	75.8769	93.4979	3700	1108.5	5.30	0.4133

Table 5. Load current THD Variations

Technique	% THD				
	(RECT. LOAD)	(R-LOAD)	(RL-LOAD)	(RLC-LOAD)	(DYNAMIC LOAD)
Without Filter	7.48	5.07	5.45	8.91	8.07

SAPF with Conv. PI	7.45	5.07	5.44	8.91	8.07
GSA	7.44	5.06	5.44	8.91	8.07
PSO	5.74	4.85	4.73	4.44	4.88
PPFO	2.38	3.71	3.22	3.89	4.07
nm-PPFO	1.99	4.34	4.33	4.33	5.22

Table 6. Source current THD Variations

Technique	% THD				
	(RECT. LOAD)	(R-LOAD)	(RL-LOAD)	(RLC-LOAD)	(DYNAMIC LOAD)
Without Filter	3.23	2.82	3.13	4.27	4.01
SAPF with Conv. PI	3.19	2.43	2.49	3.53	3.31
GSA	3.18	2.47	2.64	3.98	3.80
PSO	2.01	2.21	2.23	2.18	2.37
PPFO	1.21	2.07	2.20	2.11	2.23
Nm-PPFO	0.76	1.97	2.07	2.12	2.55

Three phase waveforms:-

CASE:-1 :(Rectifier Load)

Three Phase Waveform

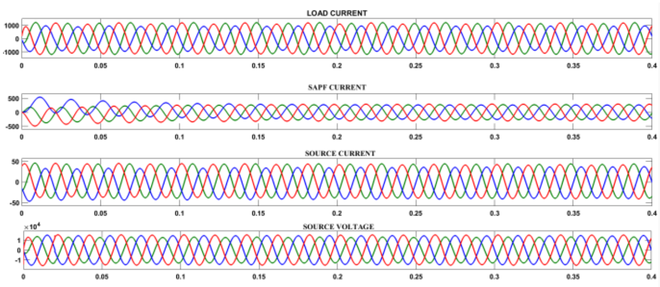

Fig. 5. (A) Iload (B) Iapf (C) Isource (D) Vsource

Load current THD

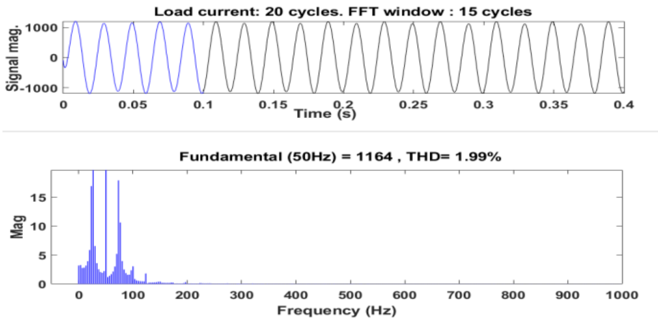

Fig. 6. Load current THD analysis

Source current THD

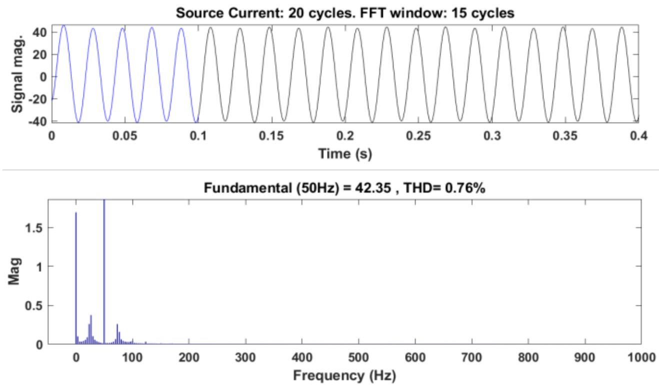

Fig. 7. Source current THD analysis

CASE:-2(R-Load)

Three Phase Waveform

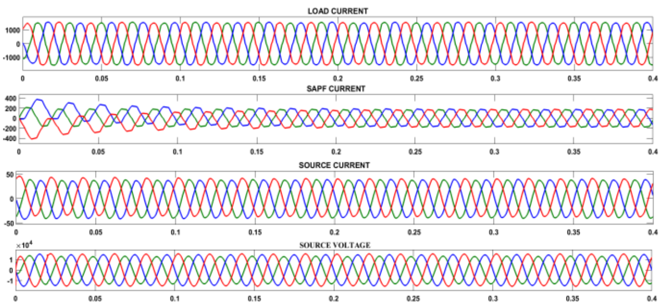

Fig. 8. (A) Iload (B) Iapf (C) Isource (D) Vsource

Load current THD

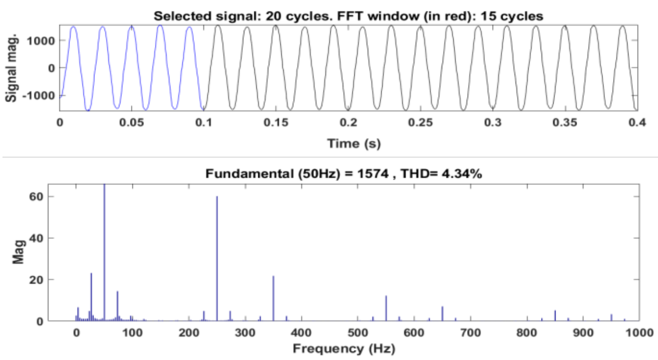

Fig. 9. Load current THD analysis

Source current THD

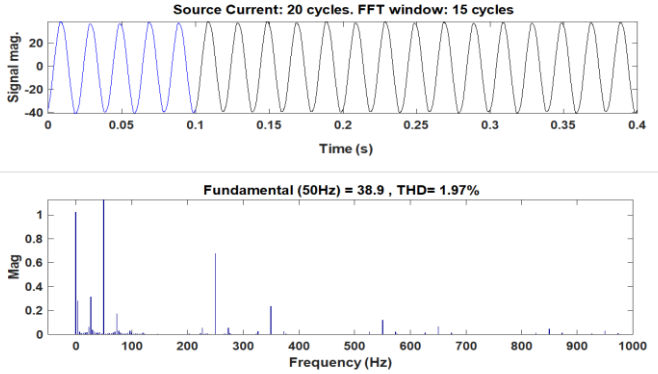

Fig. 10. Source current THD analysis

CASE:-3(RL-Load)

Three Phase Waveform

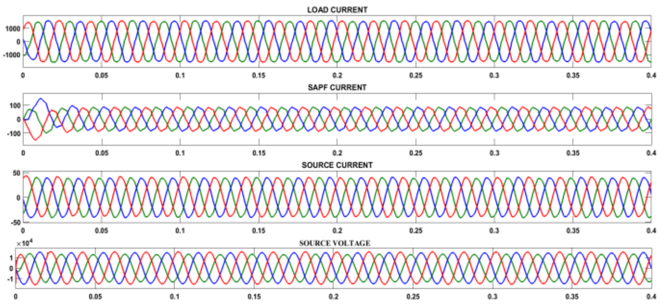

Fig. 11. (A) Iload (B) Iapf (C) Isource (D) Vsourrce

Load current THD

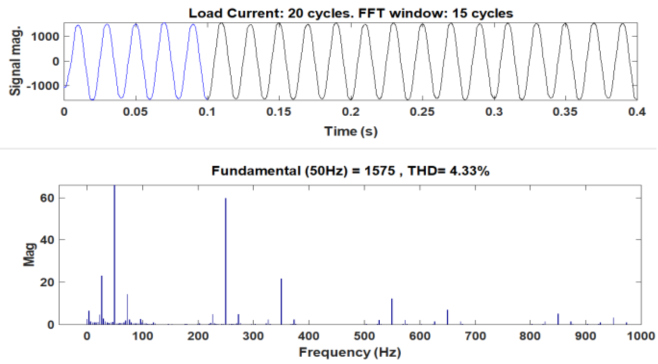

Fig. 12. Load current THD analysis

Source current THD

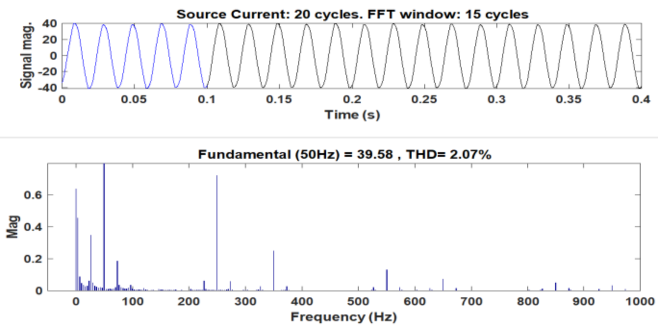

Fig. 13. Source current THD analysis

CASE:-4(RLC-Load)

Three Phase Waveform

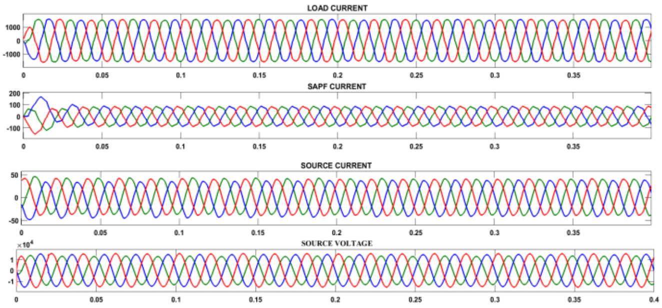

Fig. 14. (A) Iload (B) Iapf (C) Isource (D) Vsource

Load current THD

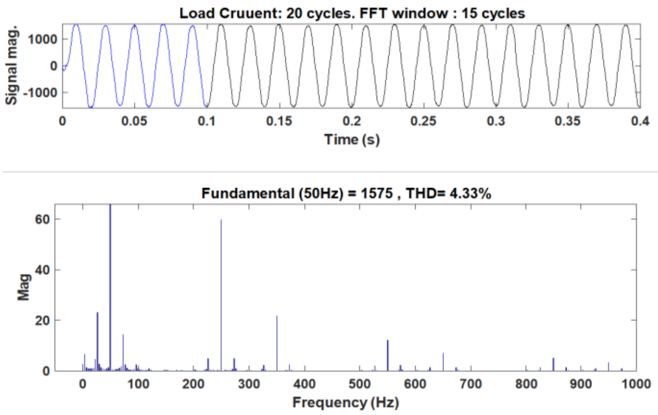

Fig. 15. Load current THD analysis

Source Current THD

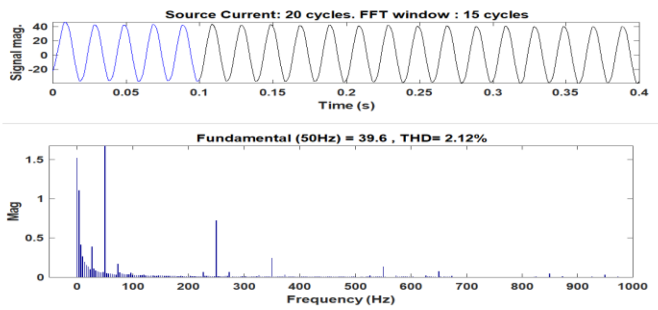

Fig. 16. Source current THD

CASE:-5(Dynamic-Load)

Three phase waveform

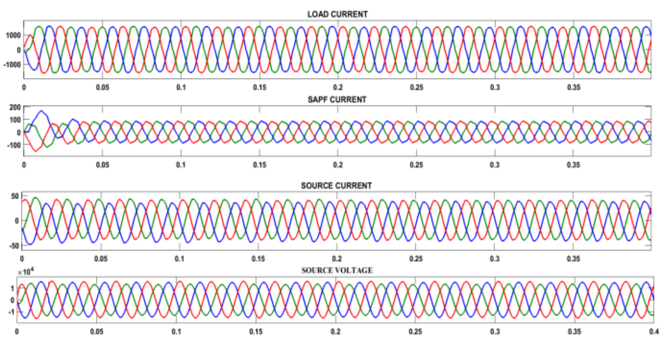

Fig. 17. (A) Iload (B) Iapf (C) Isource (D) Vsource

Load Current THD

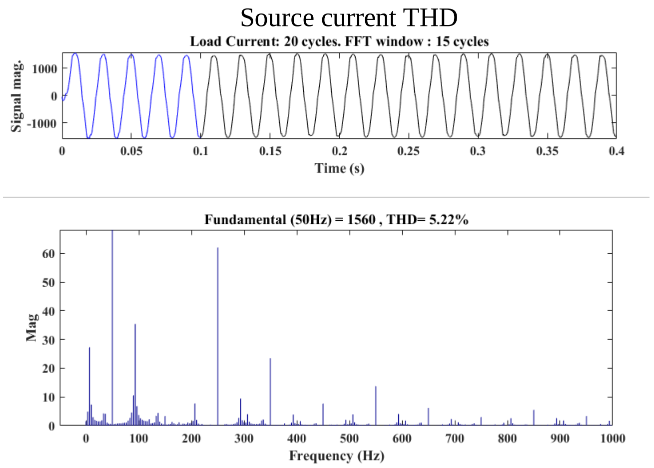

Fig. 18. Load current THD analysis

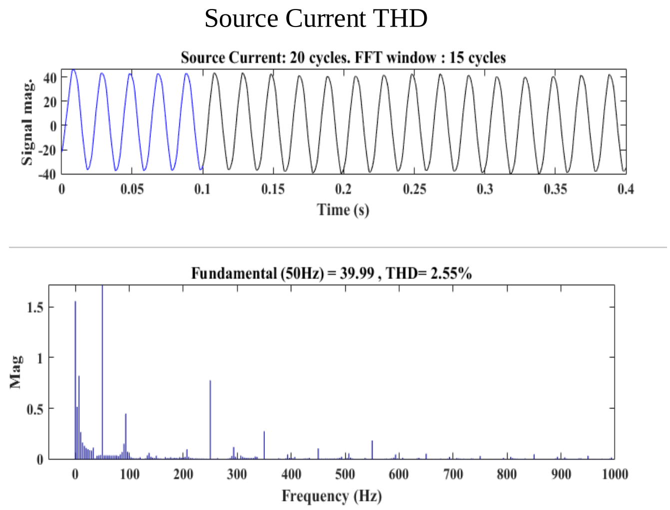

Fig. 19. Source current THD analysis

Table 7. Power factors

Test Case	No Filter			Technique	With shunt active power filter		
	Ph. a	Ph. b	Ph. c		a	b	c
1	0.9658	0.9657	0.9657	nm-PPFO	0.9996	0.9995	09996
				PPFO	0.9996	0.9994	0.9996
				FFO	0.9986	0.9981	0.9986
				GSA	0.9995	0.9994	0.9995
				PSO	0.9937	0.9948	0.9939
2	0.8995	0.9195	0.9625	nm-PPFO	0.9432	0.9448	0.9724
				PPFO	0.9932	0.8741	0.9911
				GSA	0.9933	0.8745	0.9925
				PSO	0.9934	0.9928	0.9927
3	0.9461	0.8995	0.9495	nm-PPFO	0.9991	0.9954	0.9973
				PPFO	0.9931	0.9754	0.9923
				GSA	0.9771	0.9913	0.9912
				PSO	0.9930	0.8756	0.9923
4	0.8910	0.8805	0.8910	nm-PPFO	0.9929	0.9726	0.9926
				PPFO	0.9929	0.9726	0.9926
				GSA	0.9929	0.9726	0.9926
				PSO	0.9928	0.9726	0.9926
5	0.8996	0.8991	0.8996	Nm-PPFO	0.9978	0.9987	0.9981
				PPFO	0.9925	0.9872	0.9927
				GSA	0.9927	0.9814	0.9928
				PSO	0.9945	0.9875	0.9927

Table 8. Design parameters

Case	Method	Kp	Ki	Cdc	Vdcref	Lf	Rf
CASE-1	nm-PPFO	7.3949	9.3844	5000	1106.5	5.3	0.4123
	PPFO	75.8767	75.1039	5000	1231.06	7.334	0.2139
	GSA	19.5072	46.3490	3300	447.7925	5.8	0.1626
	PSO	0.0017	65.663	4800	1085.1	0.2615	0.3729
CASE-2	nm-PPFO	37.2953	31.4502	1300	1171.8	4.2	0.3082
	PPFO	27.824	59.8741	1291	873.65	3.95	0.2136
	GSA	88.8405	43.6745	2300	1495.6	5.6	0.2415
	PSO	62.2056	23.9917	4800	492.87	9.1	0.4346
CASE-3	nm-PPFO	98.5237	89.0036	3800	579.188	2.9	0.4817
	PPFO	70.0147	74.0013	2910	846.188	3.49	0.4324
	GSA	57.7009	64.7746	610.48	517.4380	6.059	0.1460
	PSO	1.5404	64.7746	4700	806.1715	4.0	0.2876
CASE-4	nm-PPFO	89.6405	86.7883	4600	1146.7	8.1	0.4249
	PPFO	81.5901	32.013	4600	1421.3	8.03	0.3142
	GSA	47.9110	36.0929	1300	948.4848	7.4	0.4867
	PSO	6.0363	38.4944	2300	722.9112	6.7	0.2404
CASE-5	nm-PPFO	1.1169	43.0987	3100	724.9027	8.5	0.1100
	PPFO	7.442	57.8532	3700	849.341	5.2	0.2182
	GSA	60.8102	73.3013	2300	510.174	4.9	0.3155
	PSO	88.7803	98.7959	4600	641.0308	3.4	0.3008

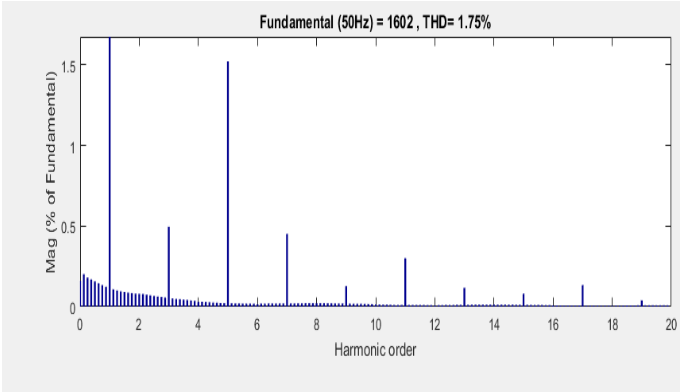

Fig. 20. Current harmonic spectrum for case-3

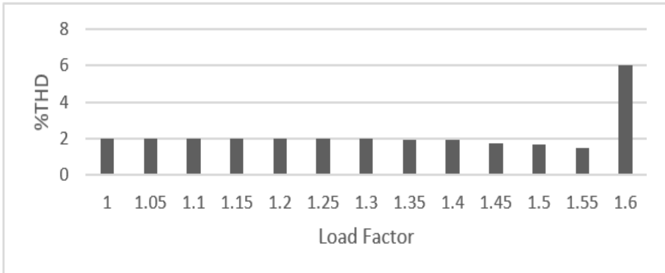

Fig. 21. THD VS. LOAD FACTOR for test case-1

Convergence characteristics of various optimization techniques:

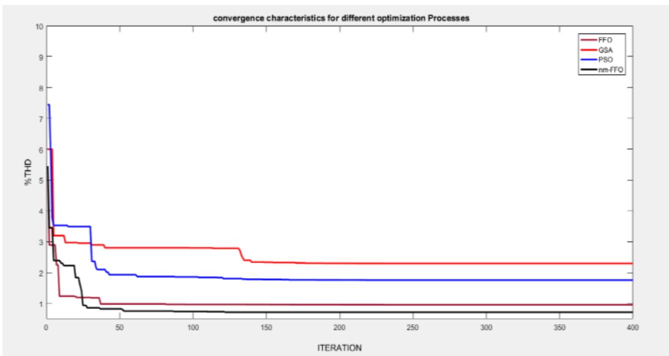

Fig. 22. Convergence characteristics for different optimization techniques

5. Conclusion

The proposed model is simulated successfully using different optimization techniques for different load levels with different test cases. The PPFO algorithm which is being developed by combining the firefly optimization technique and predator –prey concept is found to be best for optimizing the decision parameters aiming for minimization of THD and obtaining better power quality. The SAPF design is being taken as the means of optimization with an objective of reduction of THD where the PI controller gain parameters, inductance of filter and resistance, DC capacitance and DC reference voltage are taken as the decision variable which are to be optimized. Different improved optimization techniques have been applied for optimizing the problem formulated for five different test cases and it is found that nm-PPFO is the most appropriate technique which improves the THD best among all for generating sinusoidal source current. The nm-PPFO decreases the THD to the lowermost values, which are much lower as compared to contemporary optimization techniques. The THDs at the resulting source currents follow the regulations of IEEE-519-2014 standards .The proposed nm-PPFO Optimization act performs better even in unbalanced load conditions.

References

[1] AA Patil, RN Katkar, PA Ajit, CP Vijay, PP Patil, SV Patil. "Harmonic mitigation using Passive Filter "International Journal of Engineering Trends and Technology, Vol. 45.2, pp. 83-86, 2017. (Article)

[2] A Bhattacharya, C Chakraborty, "A shunt active power filter with enhanced performance using ANN-based predictive and adaptive controllers." IEEE transactions on industrial electronics, Vol. 58.2, pp. 421-428, 2010. (Article)

[3] FZ Peng, GW Ott, DJ Adams, "Harmonic and reactive power compensation based on the generalized instantaneous reactive power theory for three-phase four-wire systems." IEEE Transactions on Power Electronics, Vol. 13.6, pp. 1174-1181, 1998.(Article)

[4] RS Herrera, P Salmerón, "Instantaneous reactive power theory: A reference in the nonlinear loads compensation." IEEE Transactions on Industrial Electronics, Vol. 56.6, pp. 2015-2022, 2009.(Article)

[5] A Chebabhi, MK Fellah, A Kessal, MF Benkhoris "Comparative study of reference currents and DC bus voltage control for Three-Phase Four-Wire Four-Leg SAPF to compensate harmonics and reactive power with 3D SVM." ISA transactions, Vol. 57, pp. 360-372, 2015.(Article)

[6] P Garanayak, G Panda, PK Ray, "Harmonic estimation using RLS algorithm and elimination with improved current control technique based SAPF in a distribution network." International Journal of Electrical Power & Energy Systems, Vol. 73, pp. 209-217, 2015. (Article)

[7] AK Panda, T Penthia, "Design and modelling of SMES based SAPF for pulsed power load demands." International Journal of Electrical Power & Energy Systems, Vol. 92, pp. 114-124, 2017. (Article)

[8] K.Chandrasekaran, V.K. Ramachandaramurthy, "An improved Dynamic Voltage Restorer for power quality improvement." International Journal of Electrical Power & Energy Systems, Vol. 82, pp. 354-362, 2016.(Article)

[9] R Belaidi, A Haddouche, M Fathi, "Performance of grid-connected PV system based on SAPF for power quality improvement." 2016 International Renewable and Sustainable Energy Conference (IRSEC), pp. 542-545, IEEE, 2016. (Conference)

[10] TJ Park, GY Jeong, BH Kwon, "Shunt active filter for reactive power compensation." International Journal of Electronics, Vol. 88, pp. 121257-1269, 2001.(Article)

[11] R Hrbac, T Mlcak, V Kolar, "Improving power quality with the use of a new method of serial active power filter (SAPF) control." Elektronika ir Elektrotechnika, Vol. 23.1, pp. 15-20, 2017. (Article)

[12] GW Chang, "A new method for determining reference compensating currents of the three-phase shunt active power filter." IEEE power engineering review, Vol. 21.3, pp. 63-65, 2001. (Article)

[13] Jaber Alshehri, Ahmed Alzahrani, Muhammad Khalid, "Voltage and frequency control of micro grids with distributed generations and battery energy storage", 8th International Conference on Renewable Energy Research and Applications (ICRERA). IEEE, pp. 381-385, 2019. (Conference)

[14] Oualid Aissa, Samir Moulahoum, Ilhami Colak. "Intelligent adaptive control of the SAPF intended to improve the power grid energy quality." 2021 9th International Conference on Smart Grid (icSmartGrid). IEEE, pp. 76-81, (2021). (Conference)

[15] Alperen Mustafa Colak, Korhan Kayisli, "Reducing Voltage and Frequency Fluctuations in Power Systems using Smart Power Electronics Technologies: A Review." 2021 9th International Conference on Smart Grid (icSmartGrid). IEEE, pp. 197-200, 2021. (Conference)

[16] SR Das, PK Ray, AK Sahoo, KK Singh, "Artificial intelligence based grid connected inverters for power quality improvement in smart grid applications." Computers & Electrical Engineering, Vol. 93, p. 107208, (2021). (Conference)

[17] P Kumar, A Mahajan, "Soft computing techniques for the control of an active power filter." IEEE transactions on power delivery, Vol. 24.1, pp. 452-461.(Article)

[18] A. K. Qin, V. L. Huang, P. N. Suganthan, "Differential evolution algorithm with strategy adaptation for global numerical optimization." IEEE transactions on Evolutionary Computation. Vol. 13.2, pp. 398-417, 2008. (Article)

[19] J Liu, J Lampinen, "A fuzzy adaptive differential evolution algorithm." Soft Computing, Vol. 9.6, pp. 448-462, 2005. (Article)

[20] AP Plumb, RC Rowe, P York, M Brown, "Optimisation of the predictive ability of artificial neural network (ANN) models: a comparison of three ANN programs and four classes of training algorithm." European Journal of Pharmaceutical Sciences, Vol. 25.4-5, pp. 395-405, 2005. (Article)

[21] R Dehini, B Ferdi, B Bekkouche, "Fuzzy logic controller optimization based on GA for harmonic mitigation." Journal of Artificial Intelligence, Vol. 5.1, pp. 26-36, 2012. (Article)

[22] DH Kim, A Abraham, JH Cho, "A hybrid genetic algorithm and bacterial foraging approach for global optimization." Information Sciences, Vol. 177.18, pp. 3918-3937, 2007. (Article)

[23] Wael M. Korani, Hassel Taher Dorrah, Hassan M. Emara, "Bacterial foraging oriented by particle swarm optimization strategy for PID tuning." 2009 IEEE International Symposium on Computational Intelligence in Robotics and Automation-(CIRA), pp. 445-450, IEEE, 2009. (Conference)

[24] M Miyatake, M Veerachary, F Toriumi, "Maximum power point tracking of multiple photovoltaic arrays: A PSO approach." IEEE Transactions on Aerospace and Electronic Systems, Vol. 47.1, pp. 367-380, 2011. (Article)

[25] M Dorigo, V Maniezzo, A Colorni, "Ant system: optimization by a colony of cooperating agents." IEEE Transactions on Systems, man, and cybernetics, Part B: Cybernetics, Vol. 26.1, pp. 29-41, 1996. (Article)

[26] E Rashedi, H Nezamabadi-Pour, S Saryazdi, "GSA: a gravitational search algorithm." Information sciences, Vol. 179.13, pp. 2232-2248, 2009.

[27] S Bhaskaran, R Varma, J Ghosh, "A comparative study of GA, PSO and APSO: Feed point optimization of a patch antenna." International Journal of Scientific and Research Publications, Vol. 3.5, pp. 1-5, 2013. (Article)

[28] Gundala Srinivasa Rao, B. Srikanth Goud, Ch. Rami Reddy, "Power Quality Improvement using ASO Technique." 9th International Conference on Smart Grid (icSmartGrid). IEEE, pp. 238-242, 2021. (Conference)

[29] S Choudhury, SK Acharya, RK Khadanga, S Mohanty, "Harmonic Profile Enhancement of Grid Connected Fuel Cell through Cascaded H-Bridge Multi-Level Inverter and Improved Squirrel Search Optimization Technique." Energies, Vol. 14.23, pp. 7947, 2021. (Article)

[30] Devi Prasad Acharya, Subhashree Choudhury, Niranjan Nayak, "Photovoltaic Cell Based Shunt Active Filter and Power Quality Improvement Using Hybrid Optimization Technique." 2019 International Conference on Intelligent Computing and Remote Sensing (ICICRS). IEEE, pp.1-6, 2019. (Conference)

[31] JC Bansal, SS Jadon, R Tiwari, D Kiran, "Optimal power flow using artificial bee c olony algorithm with global and local neighbourhoods." International Journal of System Assurance Engineering and Management, Vol. 8.4, pp. 2158-2169, 2017. (Article)

[32] AAZ Diab, HM Sultan, IS Mohamed, "Application of different optimization algorithms for optimal sizing of PV/wind/diesel/battery storage stand-alone hybrid microgrid." IEEE Access 7, pp. 119223-119245, 2019. (Article)

[33] Mehmet Yesilbudak, Salih Ermis, Ramazan Bayindir, "Investigation of the effects of FACTS devices on the voltage stability of power systems." 2017 IEEE 6th International Conference on Renewable Energy Research and Applications (ICRERA), pp. 1080-1085, IEEE, 2017. (Conference)

[34] R Shigenobu, A Nakadomari, YY Hong, P Mandal, "Optimization of voltage unbalance compensation by smart inverter." Energies, Vol. 13.18, pp. 4623, 2020. (Article)

[35] S Mohammadi, B Mozafari, S Solimani, T Niknam, "An Adaptive Modified Firefly Optimisation Algorithm based on Hong's Point Estimate Method to optimal operation management in a microgrid with consideration of uncertainties." Energy, Vol. 51, pp. 339-348, 2013. (Article)

[36] A Gálvez, A Iglesias, "New memetic self-adaptive firefly algorithm for continuous optimisation." International Journal of Bio-Inspired Computation, Vol. 8.5, pp. 300-317, 2016. (Article)

[37] R Khatibi, MA Ghorbani, FA Pourhosseini, "Stream flow predictions using nature-inspired Firefly Algorithms and a Multiple Model strategy–Directions of innovation towards next generation practices." Advanced Engineering Informatics, Vol. 34, pp. 80-89, 2017. (Article)

[38] S Nandy, PP Sarkar, A Das, "Analysis of a nature inspired firefly algorithm based back-propagation neural network training." arXiv preprint arXiv: 1206.5360, 2012. (Article)

[39] SL Tilahun, HC Ong, JMT Ngnotchouye, "Extended prey-predator algorithm with a group hunting scenario." Advances in Operations Research, 2016. (Article)

[40] Mahaboob, Sahithullah, Senthil Kumar Ajithan, and Sasikala Jayaraman. "Optimal design of shunt active power filter for power quality enhancement using predator-prey based firefly optimization." Swarm and evolutionary computation, Vol. 44, pp.522-533, 2019. (Article)

[41] SR Das, PK Ray, AK Sahoo, G Dhiman, "Application of optimisation technique in PV integrated multilevel inverter for power quality improvement." Computers & Electrical Engineering, p. 107606, 2021. (Article)

[42] YKSS Rao, BB Krishna, "Modelling diesel engine fuelled with tamanu oil-Diesel blend by hybridizing neural network with firefly algorithm." Renewable Energy, Vol. 134, pp. 1200-1212, 2019. (Article)